Depth profiling of the elemental surface composition of the oral microorganism S. salivarius HB and fibrillar mutants by X-ray photoelectron spectroscopy

van der Mei, H. C.; Handley, P. S.; Busscher, H. J.

Published in:
Cell Biochemistry and Biophysics

DOI:
10.1007/BF02782657

Publication date:
1992

0163-4992/93/20/99–110/$2.20

Depth Profiling of the Elemental Surface Composition of the Oral Microorganism *S. Salivarius* HB and Fibrillar Mutants by X-Ray Photoelectron Spectroscopy

H. C. VAN DER MEI,*[,1]
P. S. HANDLEY,[2] AND H. J. BUSSCHER[1]

[1]*Laboratory for Materia Technica, University of Groningen, Antonius Deusinglaan 1, 9713 AV Groningen, The Netherlands; and* [2]*Department of Cell and Structural Biology, Stopford Building, University of Manchester, Oxford Road, Manchester M13 9PT, England*

Received February 14, 1992; Accepted July 20, 1992

ABSTRACT

X-ray photoelectron spectroscopy (XPS) on microbial cell surfaces requires freeze-drying of cells, and as a result, the cell surface appendages flatten out on the cell surface and form a collapsed fibrillar mass. At present, it is unclear how the density, length and composition of these fibrils influence the elemental surface composition as probed by XPS. The sampling depth of XPS can be varied by changing the electron take-off angle. In this article, we made a depth profiling of the collapsed fibrillar mass of *Streptococcus salivarius* HB and fibril-deficient mutants by angle-dependent XPS. Methylamine tungstate negative staining and ruthenium red staining followed by sectioning revealed distinct classes of fibrils with various lengths on each of the strains. Interpretation of the angle dependence of the oxygen/carbon (O/C) and phosphorus/carbon (P/C) surface concentration ratios of these

*Author to whom all correspondence and reprint requests should be addressed.

strains was difficult. However, the angle dependence of the nitrogen/carbon (N/C) surface concentration ratio could be fully interpreted:

N/C did not vary with sampling depth on a bald strain, *S. salivarius* HBC12 and on *S. salivarius* HB7, a strain with a dense array of fibrils of uniform length.

N/C decreased with sampling depth in case of a sparsely fibrillated strain, *S. salivarius* HBV51 and eventually reached the value observed for the bald strain, HBC12.

A high N/C at small sampling depth was observed for *S. salivarius* HB with protruding, protein rich fibrils.

We conclude that elemental depth profiling of microbial cell surfaces by XPS can be interpreted to coincide with structural and biochemical information on the cell surface as obtained by electron microscopy and can therefore be considered as a useful technique to study structural features of cell surfaces in combination with electron microscopy.

Index Entries: *S. salivarius*; surface composition; X-ray photoelectron spectroscopy; fibrils; depth profiling; oral streptococci.

INTRODUCTION

In recent years, X-ray photoelectron spectroscopy (XPS) has become a valuable tool for studying the chemical composition of the outermost surfaces of microbial cells *(1,2)*. The technique has been applied on brewery yeasts *(3,4)*, oral streptococci *(5,6)*, staphylococci *(7)*, and dairy stains *(8)*. The high vacuum (10^{-8}–10^{-9}torr) required for XPS experiments, necessitates freeze-drying of the cells therefore bringing them into a state remote from their physiological one. This can be considered as a drawback of the technique.

Despite the above, the electrophoretic behavior of a number of microbial strains could be explained on the basis of the overall chemical surface composition of the strains as probed by XPS *(4–6,9)*. High isoelectric points, i.e., the pH at which positive and negative charges are in counterbalance, were found to be caused by high N/C surface concentration ratios. Oppositely, low isoelectric points were caused predominantly by phosphate-containing groups, as concluded from high P/C and O/C surface concentration ratios of strains.

The chemical surface composition of microbial cells as probed by XPS has also been related to their cell-surface hydrophobicity, as assessed by water contact angles *(4–7)*. These studies revealed that oxygen-containing groups were responsible for their hydrophobic character. Thus, it can be concluded that despite freeze-drying of cells, XPS data bear a clear relationship with cell-surface properties existing under more physiological conditions.

The depth of the area, sampled by XPS, can be varied by changing the electron take-off angle, i.e., the angle under which electrons ejected from the

surface are detected. By varying the electron take-off angle, a depth profiling of the surface region can be obtained over approx 1–10 nm *(10)*. Bacterial cell surfaces are not smooth and usually carry structures that can either be fibrils, fimbriae, or pili *(11)*, with lengths up to 400 nm for fibrils and up to several micrometers for fimbriae, and that can be visualized by negative staining or ruthenium red staining in the transmission electron microscope. In addition, the chemical compositions of these structures may vary over their length. It is unclear how these structures on bacterial cell surfaces behave under freeze-drying. Generally, it is assumed that these structures flatten out on the cell surface, creating a collapsed mass of surface appendages. Taking these problems into consideration, it is perhaps surprising that elemental surface concentration ratios as probed by XPS, usually done at an intermediate electron take-off angle of 45°, show relationships with other cell-surface properties *(4–6,9)*.

The aim of this study was to determine whether surface structures seen in the uncollapsed state by electron microscopy correlate with the elemental surface concentration ratios taken at different depths into the cell surface after freeze-drying. In order to do this, we used the oral microorganism *Streptococcus salivarius* HB and a series of fibril-deficient mutants, for purpose of comparison. The structural features of these strains are well known through transmission electron microscopy of stained cells *(12,13)*, and the position of antigens on these structures has been localized by immunoelectron microscopy *(13)*. The chemical composition of these purified antigens has been determined by Weerkamp and Jacobs *(14)*.

MATERIALS AND METHODS

Bacterial Strains and Growth Conditions

S. salivarius HB and its mutant strains HBV5, HB7, HBV51, and HBC12 have been described previously with regard to the antigenic composition of their cell wall, and the presence or absence of surface appendages *(13,14)*. For each experiment, the bacteria were grown overnight at 37°C from a frozen stock in batch culture in Todd Hewitt broth. This culture was used to inoculate a second culture, which was grown for 16 h and then harvested by centrifugation for 10 min at 5000 × *g* and washed twice with demineralized water. A small portion of the cells was suspended in water for studying their cell-surface structures by transmission electron microscopy. The other part of the cellular pellet was frozen in a stainless-steel box in liquid nitrogen and lyophilized at 5°C in a Lyovac GT1 (Leybold Heraeus).

X-Ray Photoelectron Spectroscopy (XPS)

XPS on bacterial cell surfaces has been done essentially as described by Amory et al. *(3)*. Briefly, the freeze-dried bacterial powder was placed in a

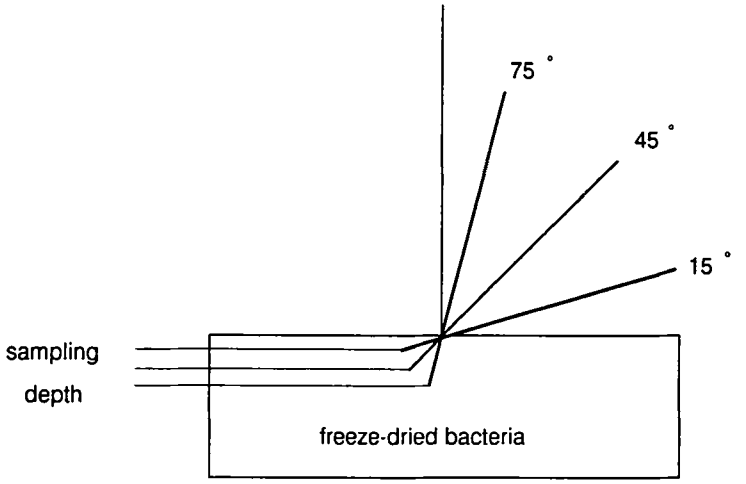

Fig. 1. Definition of the electron take-off angles used for the different sampling depths.

stainless-steel trough, and visually smooth tablets were pressed with a delrin block on top under a load of 4000 kg · m^{-2}. Subsequently, the troughs were inserted in the spectrometer, which was a Vacuum Generators ESCA MkII instrument equipped with a Tracor Northern TN 1710 signal averager for signal-to-noise ratio enhancement. A magnesium anode was used for X-ray production (14 kV, 20 mA). In order to obtain a depth profile of the collapsed fibrillar mass, different electron take-off angles were used ranging from 15 to 75° (*see* Fig. 1). The bacterial tablets, though prepared visually smooth, possess a certain roughness; hence no unique electron take-off angles exist on these substrata. In order to check whether all bacterial tablets had the same roughness, a separate series of tablets of each strain was prepared for scanning electron microscopy. XPS peaks were recorded in the following order: C_{1s}, O_{1s}, N_{1s}, and P_{2p} for 45°, and then the same series for 15 and 75° take-off angles. The C_{1s} and O_{1s} peaks were recorded again afterward at a 45° take-off angle in order to determine possible radiation-induced changes in cell-surface composition. The area under each peak after linear background subtraction was used for calculation of the peak intensities, yielding elemental surface concentration ratios O/C, N/C, and P/C employing sensitivity factors determined by Wagner et al. *(15)*. All XPS experiments were done in triplicate on cells of separate bacterial cultures.

Electron Microscopy

Transmission electron microscopy was used in order to reveal surface appendages on the cells. For negative staining, washed cells were stained in 1% methylamine tungstate on carbon-coated, hydrophilic grids in order to detect the surface fibrils as described by Handley *(16)*. Ruthenium red staining was achieved by fixation in a mixture of osmium tetroxide and ruthenium red,

followed by dehydration, embedding and sectioning in order to detect carbohydrate-rich layers (so-called RR layers) as described by Luft *(17)* and Handley *(12,18)*. All samples were studied in a Hitachi H600 transmission electron microscope operated at 100 kV.

The series of pressed bacterial tablets made for scanning electron microscopy were first kept 24 h in osmium-tetroxide saturated vapor and subsequently sputter-coated with gold. All samples were studied in a Jeol 35C scanning electron microscope operated at 25 kV.

RESULTS

Figure 2 presents the surface appendages revealed by transmission electron microscopy on both negatively stained (left panel) and ruthenium red stained (right panel) cells. The parent strain *S. salivarius* HB and the mutant HBV5 show a dense fibrillar layer after negative staining (Figs. 2a,c). The density and number of different types of fibrils decrease on HB7 (Fig. 2e) and HBV51 (Fig. 2g), whereas the mutant HBC12 is completely bald (Fig. 2i). Ruthenium red staining also reveals the different types of fibrils (Figs. 2b,d,f and h), which indicates that these fibrils consist at least partly of carbohydrates. The bald mutant HBC12 has a thin carbohydrate-rich layer on its surface (Fig. 2j) as shown by ruthenium red staining. C, O, N, and P are the only elements observed on the surfaces, and Table 1 summarizes the N/C, O/C, and P/C surface concentration ratios of the *S. salivarius* strains for various electron take-off angles as obtained by XPS. The parent strain HB and the mutant HBV51 demonstrate a decrease in the N/C surface concentration ratio when the sampling depth increases, whereas HBV5 shows a slight increase. The elemental surface concentration ratios of the mutants HB7 and HBC12 are similar for all sampling depths. The O/C surface concentration ratio decreases for all strains with increasing sampling depth, except for the mutant HBV5. The P/C surface concentration ratio shows an increase with increasing sampling depth for all strains, except for the bald mutant HBC12.

The intensities of the C_{1s} and O_{1s} peaks, recorded at a 45° electron take-off angle, changed slightly during the course of an experiment. The C_{1s} peak intensity increased by 2.4% on an average, whereas the O_{1s} peak intensity decreased by 2.6% on an average.

Scanning electron microscopy showed that the macroscopic roughness of the pressed, bacterial tablets was identical for all strains. Figure 3 presents three examples of the appearance of the surfaces of these bacterial tablets.

DISCUSSION

In this article, we measured the elemental surface composition of *S. salivarius* HB and fibrillar mutants at different sampling depths by XPS in order to

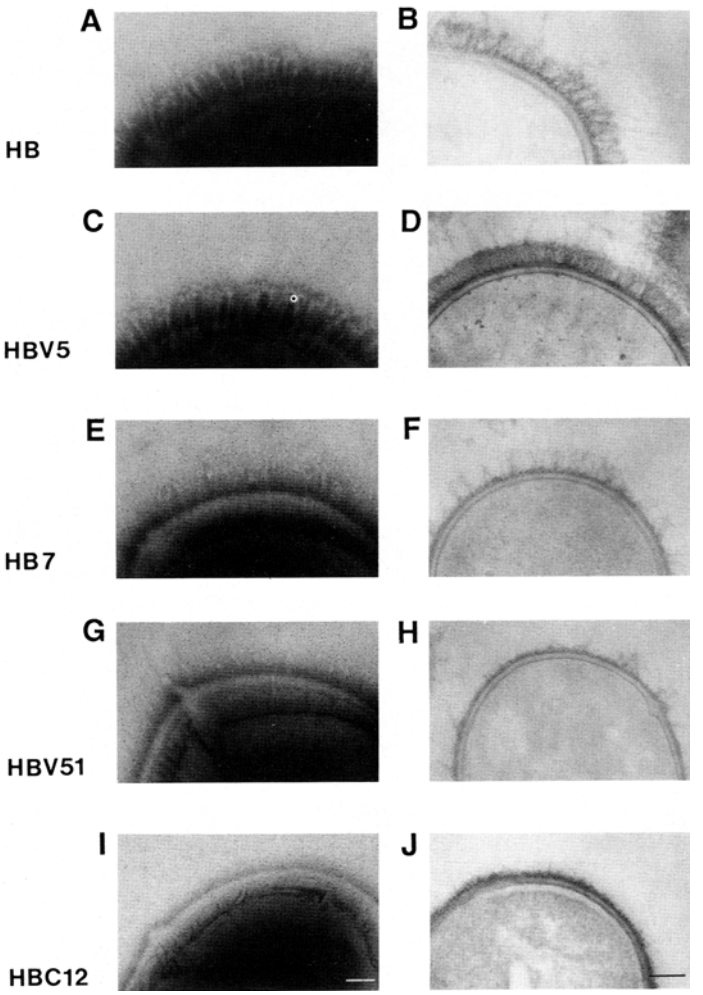

Fig. 2. Transmission electron micrographs of negatively stained (1% methylamine tungstate, left panel a, c, e, g, and i) and ruthenium red stained (right panel b, d, f, h, and j) sections of *S. salivarius* strains. The bar denotes 100 nm.

determine whether angle-dependent XPS can be used for the study of structural features of bacterial cell surfaces.

A unique electron take-off angle can only be defined on smooth surfaces, and on rough surfaces, a collection of angles is usually present. Since the roughness of all tablets was identical as concluded from the scanning electron micrographs (Fig. 3), it can be assumed that "sampling depth" increases with the electron take-off angle. For smooth surfaces, a variation in electron take-off angle from 15–75° would correspond approximately with 1–10 nm in sampling depth *(10)*. For rough substrata, the variation in sampling depth cannot be exactly given.

Table 1

Depth Profiling of the Elemental Surface Concentration Ratios of *S. salivarius* HB and Fibrillar Mutants as Obtained by XPS Carried Out at Different Electron Take-Off Angles[a]

	15°	45°	75°
N/C[b]			
S. salivarius			
HB	0.140	0.112*	0.107*
HBV5	0.086	0.107*	0.109*
HB7	0.081	0.081	0.083
HBV51	0.079	0.069	0.055
HBC12	0.057	0.054	0.057
O/C			
S. salivarius			
HB	0.603	0.485	0.507
HBV5	0.498	0.456	0.571
HB7	0.532	0.480	0.500
HBV51	0.532	0.492	0.492
HBC12	0.597	0.567	0.574
P/C			
S. salivarius			
HB	0.007	0.008	0.007
HBV5	0.003	0.005	0.006
HB7	0.002	0.006	0.009
HBV51	0.005	0.007	0.009
HBC12	0.011	0 009	0.007

[a]The standard deviations over three separate bacterial cultures amounts on an average: ±0.016 for N/C, ±0.054 for O/C, and ±0.002 for P/C.

[b]Paires analyses by a Student's *t*-test on data of separate bacterial cultures with respect to the data taken at 15° showed differences with $0.1 < p < 0.5$ for the data indicated with an asterisk.

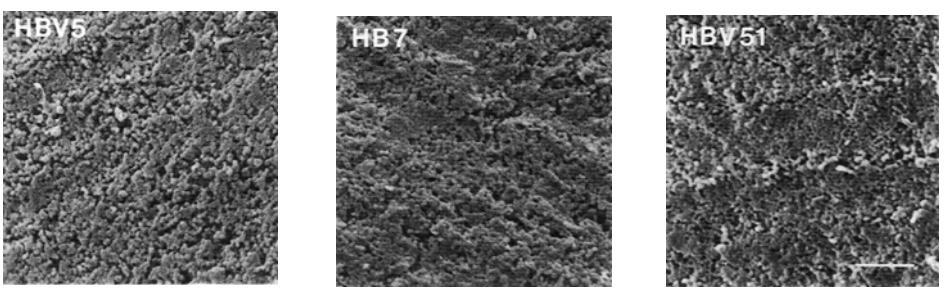

Fig. 3. Scanning electron micrographs of pressed bacterial tablets prepared for XPS of *S. salivarius* HBV5, HB7, and HBV51. The bar denotes 10 μm.

The interpretation of the data collected in Table 1 is very difficult. Previously, it had been established that interpretation of the N/C surface concentration ratio was easiest *(6,9)*, since it was related to the absence or presence of surface proteins. Interpretation of the O/C surface concentration ratio is more complex, because oxygen can be ascribed to carbohydrates, proteins, lipoteichoic acids, and so on. Furthermore, the P/C surface concentration ratio is relatively inaccurate, and interpretation of the variations observed in the P/C surface concentration ratio for these strains has not been successful so far *(5,7)*. Since nitrogen is the only element with an unambiguous interpretation, we will focus the remainder of this discussion on the angle dependence of the N/C surface concentration ratios.

The standard deviation in the N/C surface concentration ratios of the strains over three separate bacterial cultures amounts on an average: ±0.016 for N/C (*see* Table 1). Thus, it would appear that many of the variations in N/C surface concentration ratios with electron take-off angle are not significant. However, the above standard deviation is over cultures, and results taken at different angles should be compared separately for each culture. Still, paired analysis showed a small statistical significance of the differences observed in N/C surface concentration ratios (*see* Table 1). Yet, because these differences were systematically present within each culture we consider these variations with electron take-off angle meaningful to discuss. In addition, we emphasize that large differences with the electron take-off angle cannot be expected considering the structure and composition of bacterial cell surfaces.

Figures 4 and 5 present the N/C surface concentration ratios vs the electron take-off angle for all strains together with their schematic, fibrillar architecture, fibrillar length, and antigenic composition. Figure 4 demonstrates that there is a difference in the N/C surface concentration ratio at the smallest sampling depth (take-off angle of 15°) of the parent strain HB and the mutant strain HBV5. Both strains possess a dense fibrillar layer (*see also* Fig. 2), but HBV5 is lacking the fibril that is ascribed to antigen B (length 91 nm) containing 83% protein *(14)*, whereas the protein content of antigen C (length 72 nm), present on both strains, is only 57%. The sparsely distributed long fibrils (178 mn) present on both strains contain only carbohydrates and do not contribute to the N/C surface concentration ratio. The effect of the 91 nm long fibril is negligible at deeper sampling depth, as concluded from the more or less identical N/C surface concentration ratios of these strains at higher electron take-off angles. Thus, we ascribe the high N/C surface concentration ratio of HB as compared to the low N/C surface concentration ratio of HBV5 at low electron take-off angle to the presence of the 91 nm long, protein-rich, fibril.

In Figure 5, it can be seen that the N/C surface concentration ratio of HB7 does not vary over the electron take-off angle. Since this strain has only one type of fibril, we conclude that the collapsed fibrillar mass of this strain is homogeneous over the thickness of the sampling depth and, in addition, at

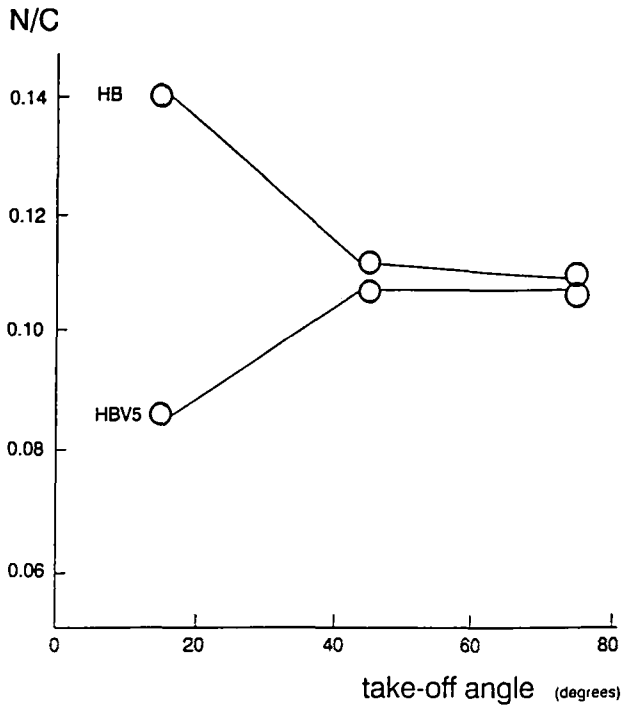

strain	antigenic composition	fibrillar architecture	fibrillar length (nm)
HB	B C D F		178 91 72
HBV5	- C D F		178 72

Fig. 4. N/C surface concentration ratios of *S. salivarius* HB and HBV5 versus the electron take-off angle (sampling depth), and a schematic summary of the structural cell-surface features of these strains *(12,13)* and their antigenic composition *(13,14)*. The protein content of antigen B, located on the 91-nm fibril is 83%, whereas the protein content of antigen C, located on the 72-nm fibril is only 57% *(14)*.

least as thick as the sampling depth. Similarly, the N/C surface concentration ratio does not vary for HBC12, although this strain is devoid of all fibrillar surface appendages. Because for this strain N/C is relatively low, we conclude that now XPS probes the RR layer, of which the composition is again constant over the various sampling depths. This is furthermore supported by the high and constant O/C surface concentration ratio.

A strong decrease in N/C surface concentration ratio with the sampling depth is shown for HBV51, starting out relatively high at a low electron take-

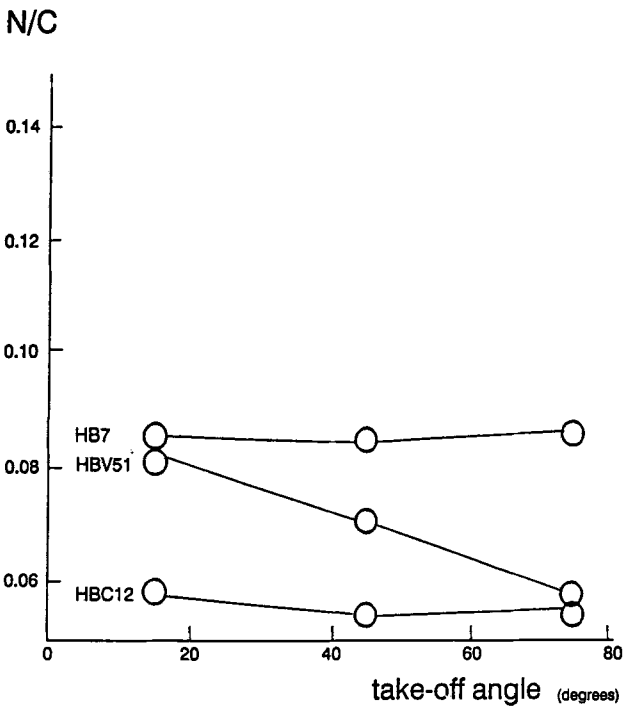

strain	antigenic composition	fibrillar architecture	fibrillar length (nm)
HB7	B - D F		91
HBV51	- - D F		63
HBC12	- - - F		

Figure 5. N/C surface concentration ratios of *S. salivarius* HB7, HBV51, and HBC12 vs the electron take-off angle (sampling depth), and a schematic summary of the structural cell-surface features of these strains *(12,13)* and their antigenic composition *(13,14)*.

off angle and decreasing to the value observed for HBC12 at the highest electron take-off angle. Thus, we conclude that the collapsed fibrillar mass of this strain, with only sparsely distributed short fibrils, is thinner than the variation in sampling depth. XPS at low electron take-off angle will probe proteinaceous appendages, but at high electron take-off angle, the influence of the sparsely distributed fibrils is negligible, and XPS will predominantly probe the underlying RR layer

Admittedly, the above discussion is based entirely on small variations with a low statistical significance. However, because all these variations can be

interpreted in terms of the known structural and biochemical features of the cell surfaces, we believe that these variations are not coincidental and thus are meaningful.

SUMMARY

In summary, it can be concluded that elemental depth profiling of microbial cell surfaces can be interpreted to coincide with structural and biochemical information on the cell surfaces as obtained by electron microscopy. However, we consider it extremely difficult at present to interpret angle-dependent XPS data fully on microbial cells in the absence of additional electron micrographs, but do not rule out that once more studies on model strains have been done, they will yield information on structural features of cell surfaces in the absence of electron micrographs that cannot be obtained by single take-off angle XPS.

ACKNOWLEDGMENTS

The authors are greatly indebted to F. Dijk (Department of Histology and Cell Biology, University of Groningen) for preparing the scanning electron micrographs, and thank Marjon Schakenraad-Dolfing for manuscript preparation.

REFERENCES

1. Amory, D. E., Genet, M. J., and Rouxhet, P. G. (1988) Application of XPS to surface analysis of yeast cells. *Surf. Interf. Anal.* **11,** 478–486.
2. Rouxhet, P. G. and Genet, M. J. (1991), Chemical composition of the microbial cell surface by X-ray photoelectron spectroscopy. *Microbial Cell Surface Analysis—Structural and Physicochemical Methods* (Mozes, N., Handley, P. S., Busscher, H. J., and Rouxhet, P. G., eds.), VCH Publishers, New York, pp. 173–220.
3. Amory, D. E., Mozes, N., Hermesse, M. P., Léonard, A. J., and Rouxhet, P. G. (1988) Chemical analysis of the surface of microorganisms by X-ray photoelectron spectroscopy. *FEMS Microbiol. Lett.* **49,** 107–110.
4. Mozes, N., Léonard, A. J., and Rouxhet, P. G. (1988) On the relations between the elemental surface composition of yeast and bacteria and their charge and hydrophobicity. *Biochim. Biophys. Acta* **945,** 324–334.
5. Van der Mei, H. C, Léonard, A. J., Weerkamp, A. H., Rouxhet, P. G., and Busscher, H. J. (1988) Properties of oral streptococci relevant for adherence: zeta potential, surface free energy and elemental composition. *Colloids and Surfaces* **32,** 297–305.
6. Busscher, H. J., Handley, P. S., Rouxhet, P. G, Hesketh, M., and Van der Mei, H. C. (1991), The relationship between structural and physicochemical sur-

face properties of tufted *Streptococcus sanguis* strains. *Microbial Cell Surface Analysis—Structural and Physicochemical Methods* (Mozes, N., Handley, P. S., Busscher, H. J., and Rouxhet, P. G., eds.), VCH Publishers, New York, pp. 317–338.

7. Van der Mei, H. C., Brokke, P., Dankert, J., Feijen, J., Rouxhet, P. G., and Busscher, H. J. (1989) Physicochemical surface properties of nonencapsulated and encapsulated coagulase-negative staphylococci. *Appl. Env. Microbiol.* **55,** 2806–2814.
8. Busscher, H. J., Bellon-Fontaine, M.-N., Mozes, N., Van der Mei, H. C., Sjollema, J., Léonard, A. J., Rouxhet, P. G., and Cerf, O. (1990) An interlaboratory comparison of physicochemical methods for studying the surface properties of microorganisms–application to *Streptococcus thermophilus* and *Leuconostoc mesenteroides. J. Microbiol. Meth.* **12,** 101–115.
9. Van der Mei, H. C., Léonard, A. J., Weerkamp, A. H., Rouxhet, P. G., and Busscher, H. J. (1988) Surface properties of *Streptococcus salivarius* HB and nonfibrillar mutants: measurement of zeta potential and elemental composition with X-ray photoelectron spectroscopy. *J. Bacteriol.* **170,** 2462–2466.
10. Ratner, B. D., Horbett, T., Shuttleworth, D., and Thomas, H. R. (1981) Analysis of the organization of protein films on solid surfaces by ESCA. *Coll. Interf. Sci.* **83,** 630–642.
11. Hammond, S. M., Lambert, P. A., and Rycroft, A. N. (1984) Surface appendages: flagella and fimbriae. *The Bacterial Cell Surface.* Kapitan Szabo, Washington DC, pp. 119–146.
12. Handley, P. S., Hargreaves, J., and Harty, D. W. (1988) Ruthenium red staining reveals surface fibrils and a layer external to the cell wall in *Streptococcus salivarius* HB and adhesion deficient mutants. *J. Gen. Microbiol.* **134,** 3165–3172.
13. Weerkamp, A. H., Handley, P. S., Baars, A., and Slot, J. W. (1986) Negative staining and immunoelectron microscopy of adhesion-deficient mutants of *Streptococcus salivarius* reveal that the adhesive protein antigens are separate classes of cell surface fibril. *J. Bacteriol.* 165, 746–755.
14. Weerkamp, A. H. and Jacobs, T. (1982) Cell wall-associated protein antigens of *Streptococcus salivarius:* purification, properties, and function in adherence. *Infect. Immun.* **38,** 233–242.
15. Wagner, C. D., Davis, L. E., Zeller, M. V., Taylor, J., Raymond, R. H., and Gale, L. H. (1981) Empirical atomic sensitivity factor for quantitative analysis by electron spectroscopy for chemical analysis. *Surf. Interf. Anal.* **3,** 211–225.
16. Handley, P. S. (1990) Structure, composition and functions of surface structures on oral bacteria. *Biofouling* **2,** 239–264.
17. Luft, J. H. (1971) Ruthenium red and violet. I. Chemistry, purification, methods used for electron microscopy and mechanism of action. *Anatomical Record* **171,** 347–368.
18. Handley, P. S. (1991) Detection of cell surface carbohydrate components. *Microbial Cell Surface Analysis—Structural and Physicochemical Methods* (Mozes, N., Handley, P. S., Busscher, H. J., and Rouxhet, P. G. eds.), VCH Publishers, New York, pp. 87–107.